LncRNA HULC regulates hepatocellular carcinoma cell proliferation, apoptosis and epithelial-mesenchymal transition via the miR-372/CXCR4 axis

Hao Liu
Wuhan NO.1 Hospital
Xiaoli Zhou
Wuhan NO.1 Hospital
Jiayao Yang
Wuhan NO.1 Hospital
Zhaohong Shi (shizhaohong7@163.com)
Wuhan No.1 Hospital

Research

Keywords: LncRNA HULC, miR-372/CXCR4 axis, hepatocellular carcinoma, proliferation, apoptosis, epithelial-mesenchymal transition

Posted Date: March 19th, 2020

DOI: https://doi.org/10.21203/rs.3.rs-18078/v1

LncRNA HULC regulates hepatocellular carcinoma cell proliferation, apoptosis and epithelial-mesenchymal transition via the miR-372/CXCR4 axis

Hao Liu, Xiaoli Zhou, Jiayao Yang, Zhaohong Shi*

Department of Gastroenterology, Wuhan NO.1 Hospital, Wuhan 430022, China

*Corresponding author: Zhaohong Shi, Department of Gastroenterology, Wuhan NO.1 Hospital. Email: shizhaohong7@163.com

Abstract

Background: Hepatocellular carcinoma (HCC) is a lethal malignancy and a major public health concern worldwide. Considering the public health risk posed by HCC, it is necessary to elucidate the mechanisms underlying liver cancer progression in order to identify more therapeutic targets. In this study, we will elucidate the role of LncRNA HULC in regulating HCC cell proliferation, apoptosis and epithelial-mesenchymal transition (EMT) via the miR-372/CXCR4 axis. **Material and Methods:** Target genes were predicted using the online TargetScan database. Cell models of gene over-expression and silencing were established by transfection, and the mRNA and protein expression levels were measured by qRT-PCR and Western blotting, respectively. Cell viability, proliferation and apoptosis were measured by the CCK-8 assay, colony formation assay and Annexin V-FITC/PI staining, respectively. *In situ* protein expression in tissues was examined by immunohistochemical staining.
Results: HULC and CXCR4 were upregulated and miR-372 was downregulated in HCC tissue and cells. TargetScan prediction and dual luciferase assay revealed that miR-372 can target HULC or CXCR4. Furthermore, HULC and CXCR4 enhanced the viability of HCC cells, whereas miR-372 had the opposite effect. Consistent with this, HULC and CXCR4 increased the proliferation of these cells and miR-372 showed an inhibitory effect. Furthermore, HULC and CXCR4 blocked apoptosis in liver cancer cells and miR-372 facilitated the same. Finally, HULC and CXCR4 promoted EMT, as indicated by E-cadherin downregulation and Vimentin upregulation, whereas miR-372 had the opposite effects.
Conclusion: HULC upregulates CXCR4 in HCC cells by inhibiting miR-372, which in turn promotes the proliferation, inhibits the apoptosis and accelerates the EMT of HCC cells.
Keywords: LncRNA HULC; miR-372/CXCR4 axis; hepatocellular carcinoma; proliferation; apoptosis; epithelial-mesenchymal transition.

Background

Hepatocellular carcinoma (HCC) is a lethal malignancy and a major public health concern worldwide[1]. Although the pathogenesis of HCC is still not fully understood, both environmental and dietary factors reportedly influence its development. Despite surgical ablation, HCC recurrence remains high and the 5-year survival of patients is less than 50%[2]. Therefore, it is crucial to understand the factors underlying HCC pathogenesis in order to identify effective diagnostic markers and therapeutic targets.

Long non-coding RNAs (LncRNA) are transcripts longer than 200 nucleotides[3] that regulate protein-encoding genes at the transcriptional, post-transcriptional and epigenetic levels, and therefore play important roles in various biological processes[4], as well as pathological states like cardiovascular diseases, inflammatory responses and cancer[5]. Several lncRNAs have been identified in HCC, such as H19, HOTAIR, MALAT1 and MEG3[6], that are potential markers for its diagnosis, prognosis and pharmacogenomics.

MicroRNAs (miRNAs) are small non-coding RNAs about 22 nucleotides long, and regulate cell proliferation, differentiation, apoptosis, protein secretion and viral infection[7]. They negatively regulate gene expression by degrading or inhibiting the translation of target messenger RNAs (mRNAs). Some miRNAs can also promote gene expression by enhancing promoter activity or translation[8]. Recent studies have shown that miRNAs play a specific role in the development and progression of liver diseases, and are thus clinically relevant for liver cancer as well[9].

C-X-C chemokine receptor 4 (CXCR4) is the specific receptor for chemokine ligand 12 (CXCL12), and promotes the development of HCC by stimulating cell proliferation, angiogenesis, invasion and metastasis[10,11]. For example, upregulation of EphA1 in HCC cells enhances the recruitment of endothelial progenitor cells (EPCs) to the tumor site, which in turn activates the SDF-1/CXCR4 axis to promote angiogenesis[12]. High CXCR4 expression in tumor endothelial cells not only induces tumor angiogenesis and facilitates metastasis, but is also correlated with the poor prognosis of HCC patients[13]. Therefore, CXCR4 is also an important factor in the development and progression of liver cancer.

In this study, we analyzed the expression pattern of lncRNAs, miRNAs and mRNAs in HCC tissues and cell lines, and examined the effects of the HULC/miR-372/CXCR4 axis on HCC cell proliferation, apoptosis and EMT. Our findings provide further insights into the molecular mechanisms underlying liver cancer, and identify HULC as a potential diagnostic biomarker and therapeutic target for HCC.

Materials and methods

Clinical tissue samples

Twenty pairs of tumor and adjacent normal liver tissues were collected from HCC patients who underwent tumor resection at our hospital, and stored at -80°C. None of the patients had received any embolization or chemotherapy before surgery, and were pathologically examined after surgery. Informed consent was provided by all patients

and the study was approved by the Ethics Committee of the hospital.

Reagents

RPMI-1640 medium, DMEM, and fetal calf serum (FCS) were purchased from Gibco. CCK-8 kit, penicillin and streptomycin were purchased from Sigma. TRIzol reagent, cDNA reverse transcription kit and SYBR Premix EX TaqTM kit were purchased from TaKaRa. MiR-372 mimics, miR-372 inhibitor and the respective negative controls (NC) were synthesized by Genepharma. PcDNA3.1-control, pcDNA3.1-HULC, si-control, si-HULC and Lipofectamine^{TM} 3000 were purchased from Invitrogen. PmirGLO vector and dual luciferase activity assay kit were purchased from Promega. Annexin V-FITC/PI kit and RIPA lysis buffer were purchased from Abcam. Mouse anti-E-cadherin, rabbit anti-Vimentin, goat anti-rabbit IgG and goat anti-mouse IgG antibodies were purchased from Cell Signaling Technology.

Cell culture

Six HCC cell lines (Huh7, Hep3B, MHCC-97L, MHCC-97H, SMMC-7721 and HepG2) and normal liver cell line (LO2) were purchased from Shanghai Institute of Biochemistry and Cell Biology, Chinese Academy of Sciences (CAS). LO2 cells were cultured in RPMI-1640 medium supplemented with 10% FCS, 100 IU/ml penicillin and 100 IU/ml streptomycin, and the HCC cell lines were cultured in complete DMEM at 37°C under 5% CO_2. The media were replaced once every two days, and healthy cells in the log phase were used for subsequent experiments.

Quantitative real time RT-PCR (qRT-PCR)

Total RNA was extracted from tissue samples or cells using TRIzol reagent, and the RNA concentration was measured by Nanodrop 2000. Equal amount of RNA per sample was reverse transcribed into cDNAs using the reverse transcription kit, followed by qRT-PCR using the SYBR Premix EX Taq^{TM} kit in the FTC-3000p cycler. U6 and β-actin were used as the internal references for HULC/miR-372 and CXCR4 respectively. Relative gene expression levels were analyzed using the $2^{-\Delta\Delta Ct}$ method. Primer sequences are shown in Table 1.

Table 1 Primer sequence

Primer	Sequence (5'-3')
HULC	Forward：5'-AGGTGGCTTGCAAAGTCAGT-3'
	Reverse：5'-AGTACTGCTTGTTCTGCCTCT-3'
miR-372	Forward：5'-ACACTCCAGCTGGGAGGUCAGGCCGAGGAC-3'
	Reverse：5'--CTCAACTGGTGTCGTGGAGTCGGCAATTCAGTTGAGAGGTCCGT-3'
CXCR4	Forward：5'-CTTCTTAACTGGCATTGTGG-3'
	Reverse：5'-GTGATGACAAAGAGGAGGTC-3'
U6	Forward：5'-GCTTCGGCAGCACATATACTAAAAT-3'
	Reverse：5'-CGCTTCACGAATTTGCGTGTCAT-3'
β-actin	Forward：5'-GAAGCTCACTGGCATGGCCTTC-3'

Reverse：5'-GACCACCTGGTGCTCAGTGTAG-3'

Cell transfection

MHCC-97L or HepG2 cells were transfected with 50 ng pcDNA3.1-control, pcDNA3.1-HULC, si-control or si-HULC and 100 nM NC, miR-372 mimics or miR-372 inhibitor using Lipofectamine according to the manufacturer's instructions. Fresh culture medium was added 6 h after transfection, and the cells were harvested 48 h later for subsequent experiments.

Dual luciferase reporter assay

The binding sites of miR-372 on the non-coding regions of HULC and CXCR4 were analyzed using the TargetScan database. For the reporter assay, HULC 3'UTR wt/mut and CXCR4 3'UTR wt/mut sequences were respectively cloned into the pmirGLO vector. The MHCC-97L or HepG2 cells were then transfected with NC, miR-372 mimics or miR-372 inhibitor, and the wt/mut HULC/CXCR4 sequences. Luciferase activity in the transfected cells was measured using the dual luciferase assay kit after 48 h.

CCK-8 assay

MHCC-97L and HepG2 cells were respectively seeded into 96-well plates at the density of 2×10^4 cells/well, and transfected as above once they were 60%-80% confluent. After 24 h, 48 h, 72 h or 96 h of culture, 10 μL CCK-8 solution was added and the cells were incubated for 2 h at 37°C. The absorbance at 450 nm was measured using an automated microplate reader.

Colony formation assay

Suitably transfected MHCC-97L and HepG2 cells were harvested after 48 h and plated onto 60 mm culture dish. The culture medium was replaced once every three days, and the ensuing colonies were stained with crystal violet after 14 days of culture. The number of colonies containing ≥50 cells were counted and photographed.

Flow cytometry

Transfected cells were harvested and resuspended in staining buffer, and sequentially stained with 10 μL each of Annexin V-FITC and propidium iodide (PI) for 30 min at room temperature in the dark. The stained cells were then analyzed using the FACSCalibur™ flow cytometer.

Immunohistochemistry

Tumor and normal liver tissues were fixed, paraffin embedded, and cut into 4 μm-thick sections. The latter were dewaxed, dehydrated and rinsed with PBS, and treated with 3% hydrogen peroxide to quench endogenous peroxidases. After blocking with non-immunized animal serum for 20 min, the sections were incubated with anti-mouse anti-E-cadherin antibody (1:200) or rabbit anti-Vimentin antibody (1:200), rinsed with PBS, and then incubated with the appropriate secondary antibody (1:200). Following another wash with PBS, the sections were incubated with ABC compound and visualized by DAB. The immuno-stained sections were examined under 400× magnification.

Western blotting

Total protein was extracted from the suitably-transfected cells with the RIPA lysis buffer and quantified using the BCA assay. Equal amount of proteins per sample were

denatured, separated by electrophoresis, and transferred onto a PVDF membrane. After blocking with 5% skim milk, the blots were incubated overnight with the primary antibodies as above at 4°C, followed by the secondary antibody (1:1000) at room temperature for 1 h. The protein bands were visualized by chemiluminescence, and analyzed using the Image-Pro Plus image analysis system.

Statistical analysis

Statistical analysis was performed using SPSS 19.0 software. Results from at least 3 independent experiments were expressed as mean ± standard deviation ($\bar{x} \pm s$). Pairwise comparison was performed using the LSD method, and multiple comparisons using the Dunnett's or Bonferroni's test after one-way ANOVA. $P<0.05$ was considered statistically significant.

Results

HULC is highly expressed in HCC tissues and cells

The qRT-PCR results showed that HULC expression was significantly higher in the HCC tissues compared to the adjacent non-tumor tissues ($P<0.01$, Figure 1A). Likewise, HULC expression was also significantly higher in all six HCC cell lines compared to that in LO2 cells. The MHCC-97L and HepG2 lines had the lowest ($P<0.05$) and highest ($P<0.001$) HULC expression levels respectively, and were thus used for subsequent gain and loss of function experiments. Taken together, HULC is overexpressed in HCC tissues and cells.

Effect of HULC on HCC cell proliferation, apoptosis and EMT

To further determine the role of HULC in HCC cells, we transfected the MHCC-97L cells and HepG2 lines with pcDNA3.1-HULC and si-HULC respectively, which significantly increased and decreased HULC expression levels (both $P < 0.01$, Figure 2A and 2B). Functionally, HULC overexpression significantly enhanced the viability of MHCC-97L cells ($P<0.01$; Figure 2C), while HULC silencing had the opposite effect ($P<0.01$, Figure 2D). Colony formation assay further revealed that HULC overexpression significantly enhanced MHCC-97L cell proliferation ($P<0.01$, Figure 2E), while its low levels decreased the number of HepG2 colonies ($P<0.01$, Figure 2F). Consistent with this, HULC overexpression showed an anti-apoptotic effect on the MHCC-97L cells ($P<0.01$, Figure 2G), while HULC silencing expression increased apoptosis in HepG2 cells ($P<0.01$, Figure 2H). In addition, the epithelial marker E-cadherin was upregulated and the mesenchymal Vimentin was downregulated in HULC-overexpressing MHCC-97L cells, whereas low levels of HULC had the opposite effect in HepG2 cells (both $P<0.01$, Figure 3A and B). Altogether, our results demonstrate that HULC promotes the proliferation and EMT of HCC cells, and blocks apoptosis.

MiR-372 is the target of HULC

To explore the potential relationship between miR-372 and HULC in HCC cells, we used the TargetScan database to identify the potential cognate binding sites (Figure 4A). In addition, we found that miR-372 was significantly downregulated in HCC tissues and cells (both $P<0.01$, Figure 4B and 4C), as well as negatively correlated with HULC expression in HCC tissues ($r = -0.56$, $P<0.001$, Figure 4D). To confirm an

interaction between the two, we transfected the MHCC-97L and Hep2G cells with miR-372 inhibitor or mimics, and accordingly verified low and high expression levels of miR-372 (both P<0.05, Figure 4E). Dual luciferase reporter assay demonstrated that miR-372 significantly inhibited the luciferase activity in cells expressing the wild-type HULC 3'UTR but not in the HULC 3'UTR mut cells (both P<0.01, Figure F). In addition, HULC downregulated miR-372 in the HCC cells (both P < 0.05, Figure 4G), and manipulating miR-372 levels significantly upregulated or downregulated HULC expression in HCC cells (both P < 0.01, Figure 4H). Taken together, these results show that HULC and miR-372 suppress each other in HCC cells via direct binding.

Effect of miR-372 on HCC cell proliferation, apoptosis and EMT

Low miR-372 expression significantly enhanced the viability of MHCC-97 cells (P<0.01), whereas miR-372 overexpression remarkably reduced that of HepG2 cells (P<0.01, Figure 5A). Consistent with this, the miR-372 inhibitor significantly enhanced MHCC-97 cell proliferation and increased the number of colonies (P<0.01), whereas miR-372 overexpression had the opposite effect on HepG2 cells (P<0.01, Figure 5B). Apoptosis was respectively promoted and blocked in HCC cells by the miR-372 mimics (P<0.01) and inhibitor (P<0.05, Figure 5C). In addition, E-cadherin was significantly downregulated and Vimentin was significantly upregulated in the miR-372 inhibitor group compared to that in the miR-372-overexpressing cells (both P < 0.01, Figure 6A, 6B). Taken together, miR-372 inhibits proliferation and EMT of HCC cells, and promotes apoptosis.

Relationship among CXCR4, miR-372 and HULC

To determine the relationship between miR-372 and CXCR4, we used the TargetScan database to predict the binding site between miR-372 and CXCR4 (Figure 7A). CXCR4 was significantly upregulated in the HCC tissues and cells (both P<0.05, Figure 7B and 7C), and negatively correlated with miR-372 expression (r = -0.415, P<0.001, Figure 7D). The dual luciferase reporter assay indicated that miR-372 inhibited luciferase activity in HCC cells transfected with CXCR4 3'UTR wt but not in cells expressing CXCR4 3'UTR mut (both P < 0.01; Figure 7E). In addition, miR-372 negatively regulated CXCR4 expression in HCC cells (both P<0.01, Figure 7F), whereas HULC had a positive regulatory effect on CXCR4 (both P<0.01, Figure 7G). Taken together, CXCR4 is a direct target of miR-372 and positively regulated by HULC in HCC cells.

HULC/miR-372/CXCR4 axis affects the proliferation, apoptosis and EMT of HCC cells

We next examined the role of the HULC/miR-372/CXCR4 axis in HCC cell proliferation, apoptosis, and EMT progression. The miR-372 mimics downregulated CXCR4 in the HULC-overexpressing cells (P<0.01), whereas inhibition of miR-372 in the HULC-silenced cells upregulated CXCR4 levels (P<0.01, Figure 8A). In addition, miR-372 overexpression reduced the viability of HULC-overexpressing cells (P<0.01), while low miR-372 expression had the opposite effect in the HULC-silenced cells (P<0.01, Figure 8B). Consistent with this, the miR-372 mimics and inhibitor respectively reversed the effects of HULC overexpression and silencing

on proliferation ($P<0.001$ for both, Figure 8C), apoptosis ($P<0.01$ and $P < 0.001$, Figure 8D) and EMT (all $P < 0.01$, Figure 8E). Together, the effect of HULC on HCC is mediated through the HULC/ miR-372/CXCR4 axis.

Discussion

HCC accounts for 75-85% of all liver cancer cases worldwide[14]. Roughly 466,100 new cases of HCC were diagnosed in China in 2015, which accounted for more than 50% of all newly diagnosed HCC cases worldwide[15]. Considering the public health risk posed by HCC, it is necessary to elucidate the mechanisms underlying liver cancer progression in order to identify more therapeutic targets.

According to the Human Genome Project, approximately 90% of the genome is transcribed into non-coding RNAs[16], which include lncRNAs and miRNAs that are the key regulators of cancer and other diseases[17,18]. In fact, lncRNAs and miRNAs are involved in almost all steps of cancer development and progression. The lncRNA HULC is associated with cancer progression[19], and plays an active role in hepatoma development by regulating lipid metabolism[20]. Furthermore, HULC enhanced EMT and promoted the metastasis of HCC cells[21]. In this study, we detected aberrantly high levels of HULC in HCC tissues and cells, which correlated to increased proliferation and EMT, and low apoptosis rates of the HCC cells. Therefore, HULC acts an oncogene in HCC, and is a potential prognostic biomarker or therapeutic target.

MiRNAs are endogenous, highly conserved, ~22 nucleotide-long non-protein-encoding RNAs that regulate target gene expression through complex pathways[22,23]. MiR-372 is a member of the Mir-371-372 gene cluster located on chromosome 19q13.42. A recent study showed that miR-372 regulates cell cycle, apoptosis, invasion and proliferation in various human cancer[24]. Lai et al.[25] found that miR-372 post-transcriptionally downregulated large tumor suppressor 2 in non-small cell lung cancer patients, thereby accelerating cancer development and proliferation of the malignant cells. However, the role of miR-372 in liver cancer is unclear. Previous reports indicate that miR-372 is expressed at low levels in HCC tissues, and its anti-tumor effect is mediated via inactivation of its target gene ATAD2[26]. Consistent with this, we also detected low miR-372 expression in HCC tissues and cells. In addition, ectopic miR-372 expression in the HCC cells significantly inhibited their proliferation and EMT, and promoted apoptosis. Therefore, miR-372 is also a potential diagnostic/prognostic biomarker of HCC.

CXCR4 is overexpressed in over 20 cancer types and plays a key role in tumor growth, invasion, microenvironment interaction, and metastasis[27]. It is often associated with adverse outcomes of various solid tumors, like breast cancer, renal cell carcinoma, gynecologic cancers, pancreatic adenocarcinoma and HCC[28]. CXCR4 was highly expressed in the HCC tissues and cells in our study as well, indicating that downregulating CXCR4 may inhibit HCC cell growth and cancer progression.

Conclusions

HULC upregulates CXCR4 in HCC cells by inhibiting miR-372, which in turn promotes the proliferation, inhibits the apoptosis and accelerates the EMT of HCC cells. Thus, the HULC/miR-372/CXCR4 axis is crucial to the progression of HCC and a promising therapeutic target. Our study illustrates for the first time an interaction between HULC, miR-372 and CXCR4 in HCC. Uncovering similar interactions among other lncRNAs, miRNAs and mRNAs in HCC will help further our understanding of the disease.

List of abbreviations

HCC: hepatocellular carcinoma (HCC); EMT: epithelial-mesenchymal transition; LncRNA: long non-coding RNAs; mRNAs: messenger RNAs; CXCR: 4C-X-C chemokine receptor 4; CXCL12: chemokine ligand 12; EPCs: endothelial progenitor cells; FCS: fetal calf serum.

Declarations

Ethics approval and consent to participate
Not applicable.
Availability of data and materials
All data are available in the included figures.
Competing interests
The authors declare that they have no conflict of interests.
Acknowledgements
None.
Consent for publication

None.

Funding
This work was supported by Natural Science Foundation of Hubei Province (2019CFB187).

Authors' contributions
Conceptualization: HL, ZS; Methodology: HL, JY; Software: XZ; Supervision: ZS; Writing original draft: HL, ZS; All authors read and approved the final manuscript.

References

1. Donadon M, Solbiati L, Dawson L, Barry A, Sapisochin G, Greig PD, Shiina S, Fontana A, Torzilli G. Hepatocellular carcinoma: the role of interventional oncology. Liver cancer 2017; 6(1): 34-43.https://doi.org/10.1159/000449346
2. Liu P-H, Hsu C-Y, Hsia C-Y, Lee Y-H, Su C-W, Huang Y-H, Lee F-Y, Lin H-C, Huo T-I. Prognosis of hepatocellular carcinoma: Assessment of eleven staging systems. Journal of hepatology 2016; 64(3): 601-608.https://doi.org/10.1016/j.jhep.2015.10.029
3. Novikova IV, Hennelly SP, Sanbonmatsu KY. Tackling structures of long noncoding RNAs. International journal of molecular sciences 2013; 14(12): 23672-23684.https://doi.org/10.3390/ijms141223672

4. Eades G, Zhang Y-S, Li Q-L, Xia J-X, Yao Y, Zhou Q. Long non-coding RNAs in stem cells and cancer. World journal of clinical oncology 2014; 5(2): 134.https://doi.org/10.5306/wjco.v5.i2.134
5. Fatica A, Bozzoni I. Long non-coding RNAs: new players in cell differentiation and development. Nature Reviews Genetics 2014; 15(1): 7-21.https://doi.org/10.1038/nrg3606
6. Sun J, Bie B, Zhang S, Yang J, Li Z. Long non-coding RNAs: critical players in hepatocellular carcinoma. International journal of molecular sciences 2014; 15(11): 20434-20448.https://doi.org/10.3390/ijms151120434
7. Wang Y, Xue J, Kuang H, Zhou X, Liao L, Yin F. microRNA-1297 inhibits the growth and metastasis of colorectal cancer by suppressing cyclin D2 expression. DNA and cell biology 2017; 36(11): 991-999.https://doi.org/10.1089/dna.2017.3829
8. Van Peer G, Mets E, Claeys S, De Punt I, Lefever S, Ongenaert M, Rondou P, Speleman F, Mestdagh P, Vandesompele J. A high-throughput 3'UTR reporter screening identifies microRNA interactomes of cancer genes. PloS one 2018; 13(3).https://doi.org/10.1371/journal.pone.0194017
9. Xiao D, Gao H. Mechanism of miR107targeting of regulator of Gprotein signaling 4 in hepatocellular carcinoma. Oncology letters 2019; 18(5): 5145-5154.https://doi.org/10.3892/ol.2019.10857
10. Ghanem I, Riveiro ME, Paradis V, Faivre S, de Parga PMV, Raymond E. Insights on the CXCL12-CXCR4 axis in hepatocellular carcinoma carcinogenesis. American journal of translational research 2014; 6(4): 340.https://doi.org/10.1016/B978-0-12-420117-0.00008-6
11. Liu H, Liu Y, Liu W, Zhang W, Xu J. EZH2-mediated loss of miR-622 determines CXCR4 activation in hepatocellular carcinoma. Nature communications 2015; 6(1): 1-15.https://doi.org/10.1038/ncomms9494
12. Wang Y, Yu H, Shan Y, Tao C, Wu F, Yu Z, Guo P, Huang J, Li J, Zhu Q. EphA1 activation promotes the homing of endothelial progenitor cells to hepatocellular carcinoma for tumor neovascularization through the SDF-1/CXCR4 signaling pathway. Journal of Experimental & Clinical Cancer Research 2016; 35(1): 65.https://doi.org/10.1186/s13046-016-0339-6
13. Xu J, Liang J, Meng Y-M, Yan J, Yu X-J, Liu C-Q, Xu L, Zhuang S-M, Zheng L. Vascular CXCR4 expression promotes vessel sprouting and sensitivity to sorafenib treatment in hepatocellular carcinoma. Clinical Cancer Research 2017; 23(15): 4482-4492.https://doi.org/10.1158/1078-0432.CCR-16-2131
14. Bray F, Ferlay J, Soerjomataram I, Siegel RL, Torre LA, Jemal A. Global cancer statistics 2018: GLOBOCAN estimates of incidence and mortality worldwide for 36 cancers in 185 countries. CA: a cancer journal for clinicians 2018; 68(6): 394-424.https://doi.org/10.3322/caac.21492
15. Chen W, Zheng R, Baade PD, Zhang S, Zeng H, Bray F, Jemal A, Yu XQ, He J. Cancer statistics in China, 2015. CA: a cancer journal for clinicians 2016; 66(2): 115-132.https://doi.org/10.3322/caac.21338
16. Rinn JL, Chang HY. Genome regulation by long noncoding RNAs. Annual review of biochemistry 2012; 81:

145-166.https://doi.org/10.1146/annurev-biochem-051410-092902
17. Qiu L, Tang Q, Li G, Chen K. Long non-coding RNAs as biomarkers and therapeutic targets: recent insights into hepatocellular carcinoma. Life sciences 2017; 191: 273-282.https://doi.org/10.1016/j.lfs.2017.10.007
18. Lakner AM, Bonkovsky HL, Schrum LW. microRNAs: fad or future of liver disease. World journal of gastroenterology: WJG 2011; 17(20): 2536.https://doi.org/10.3748/wjg.v17.i20.2536
19. Chen S, Wu D-D, Sang X-B, Wang L-L, Zong Z-H, Sun K-X, Liu B-L, Zhao Y. The lncRNA HULC functions as an oncogene by targeting ATG7 and ITGB1 in epithelial ovarian carcinoma. Cell Death & Disease 2017; 8(10): e3118.https://doi.org/10.1038/cddis.2017.486
20. Cui M, Xiao Z, Wang Y, Zheng M, Song T, Cai X, Sun B, Ye L, Zhang X. Long noncoding RNA HULC modulates abnormal lipid metabolism in Hepatoma cells through an miR-9–mediated RXRA signaling pathway. Cancer research 2015; 75(5): 846-857.https://doi.org/10.1158/0008-5472.can-14-1192
21. Li S-P, Xu H-X, Yu Y, He J-D, Wang Z, Xu Y-J, Wang C-Y, Zhang H-M, Zhang R-X, Zhang J-J. LncRNA HULC enhances epithelial-mesenchymal transition to promote tumorigenesis and metastasis of hepatocellular carcinoma via the miR-200a-3p/ZEB1 signaling pathway. Oncotarget 2016; 7(27): 42431.https://doi.org/10.18632/oncotarget.9883
22. Barshack I, Meiri E, Rosenwald S, Lebanony D, Bronfeld M, Aviel-Ronen S, Rosenblatt K, Polak-Charcon S, Leizerman I, Ezagouri M. Differential diagnosis of hepatocellular carcinoma from metastatic tumors in the liver using microRNA expression. The international journal of biochemistry & cell biology 2010; 42(8): 1355-1362.https://doi.org/10.1016/j.biocel.2009.02.021
23. Li D, Liu X, Lin L, Hou J, Li N, Wang C, Wang P, Zhang Q, Zhang P, Zhou W. MicroRNA-99a inhibits hepatocellular carcinoma growth and correlates with prognosis of patients with hepatocellular carcinoma. Journal of Biological Chemistry 2011; 286(42): 36677-36685.https://doi.org/10.1074/jbc.M111.270561
24. Voorhoeve PM, Le Sage C, Schrier M, Gillis AJ, Stoop H, Nagel R, Liu Y-P, Van Duijse J, Drost J, Griekspoor A. A genetic screen implicates miRNA-372 and miRNA-373 as oncogenes in testicular germ cell tumors. Cell 2006; 124(6): 1169-1181.https://doi.org/10.1016/j.cell.2006.02.037
25. Lai JH, She TF, Juang YM, Tsay YG, Huang AH, Yu SL, Chen JJW, Lai CC. Comparative proteomic profiling of human lung adenocarcinoma cells (CL 1â€ “0) expressing miRâ€ • 372. Electrophoresis 2012; 33(4).https://doi.org/10.1002/elps.201100329
26. Wu G, Liu H, He H, Wang Y, Lu X, Yu Y, Xia S, Meng X, Liu Y. miR-372 down-regulates the oncogene ATAD2 to influence hepatocellular carcinoma proliferation and metastasis. Bmc Cancer 2014; 14(1): 107.https://doi.org/10.1186/1471-2407-14-107
27. Walenkamp AM, Lapa C, Herrmann K, Wester H-J. CXCR4 ligands: the next big hit? Journal of Nuclear Medicine 2017; 58(Supplement 2): 77S-82S.https://doi.org/10.2967/jnumed.116.186874

28. Zhao H, Guo L, Zhao H, Zhao J, Weng H, Zhao B. CXCR4 over-expression and survival in cancer: a system review and meta-analysis. Oncotarget 2015; 6(7): 5022.https://doi.org/10.18632/oncotarget.3217

Figures

Figure 1. HULC expression in HCC tissues and cells. The results of qRT-PCR analysis showing upregulation of HULC in (A) tumor and adjacent non-tumor tissues, and (B) HCC cell lines and LO2 cells. $^{\#\#}P<0.01$ compared to adjacent non-tumor tissues, $^{*}P<0.05$, $^{**}P<0.01$ and $^{***}P<0.001$ compared to LO2 cells.

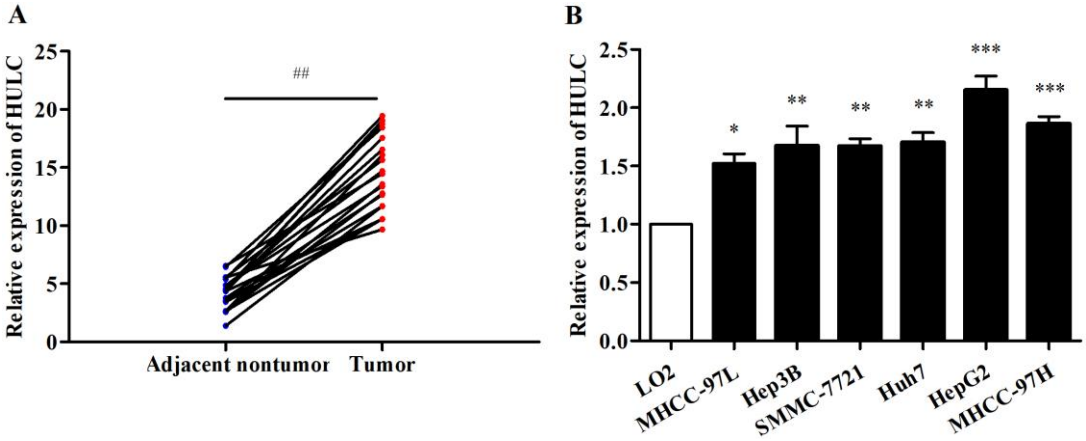

Figure 2. HULC enhances the neoplastic characteristics of HCC cells. Results of qRT-PCR analysis showing HULC expression levels in (A) MHCC-97L and (B) HepG2 cells. CCK-8 assay showing the effect of (C) pcDNA3.1-HULC and (D) si-HULC on the viability of indicated HCC cell lines. Number of colonies formed by the (E) HULC-overexpressing MHCC-97L cells and (F) HULC knockdown HepG2 cells. Flow cytometry plots showing apoptosis rates in (G) HULC-overexpressing MHCC-97L cells and (H) HULC knockdown HepG2 cells. $^{**}P<0.01$ compared with the pcDNA3.1-control group, and $^{\#\#}P<0.01$ compared with the si-control group.

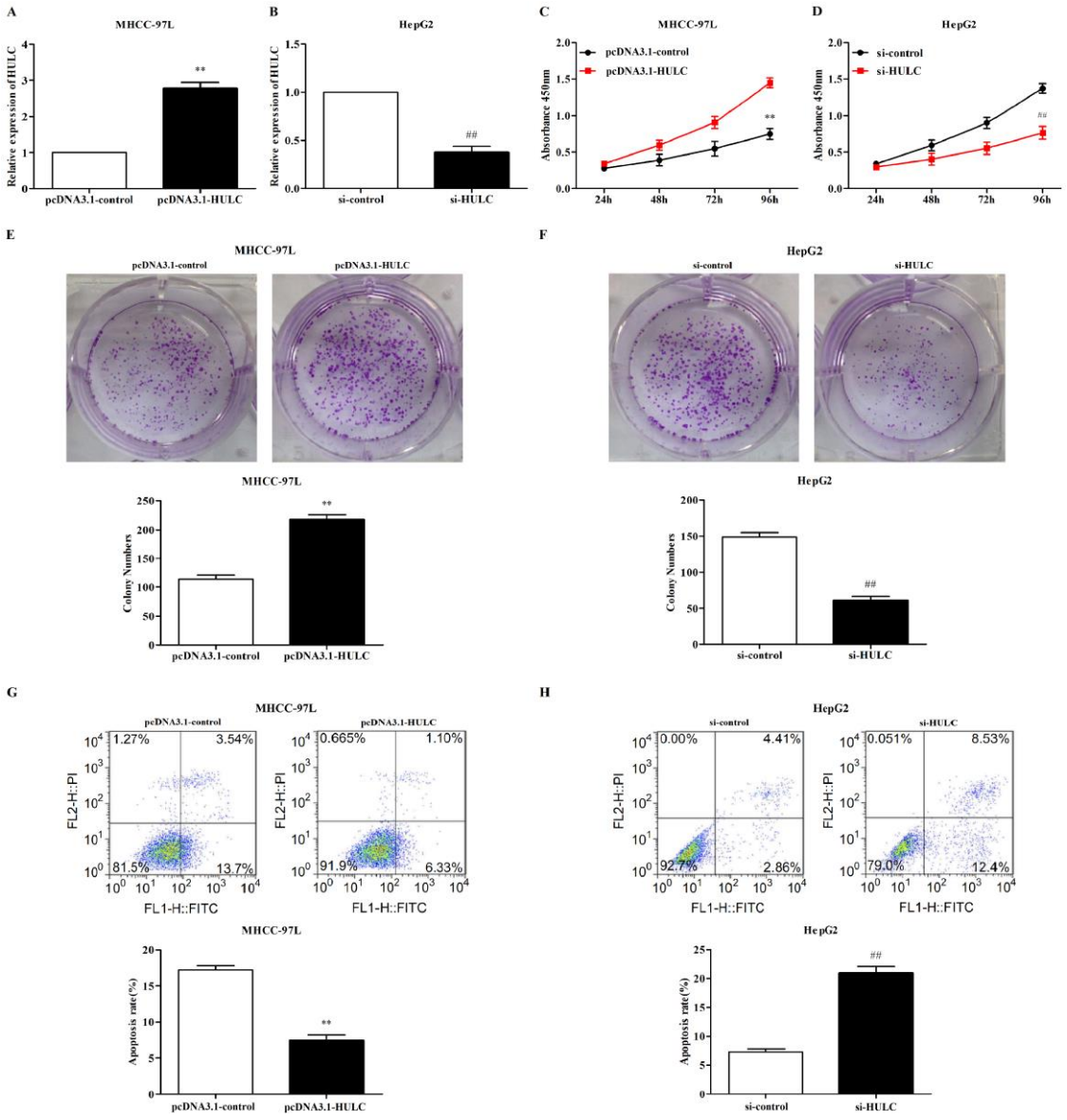

Figure 3. HULC promoted EMT progression of HCC cells. (A) Representative IHC images showing *in situ* E-cadherin and Vimentin expression in the HULC-overexpressing and HULC-knockdown HCC cells (x400). (B) Immunoblot showing expression levels of E-cadherin and Vimentin in the indicated cell lines. $^{\&\&}$P<0.01 compared to HULC^{low} group, **p<0.01 compared to pcDNA3.1-control group, and $^{\#\#}$P<0.01 compared to si-control group.

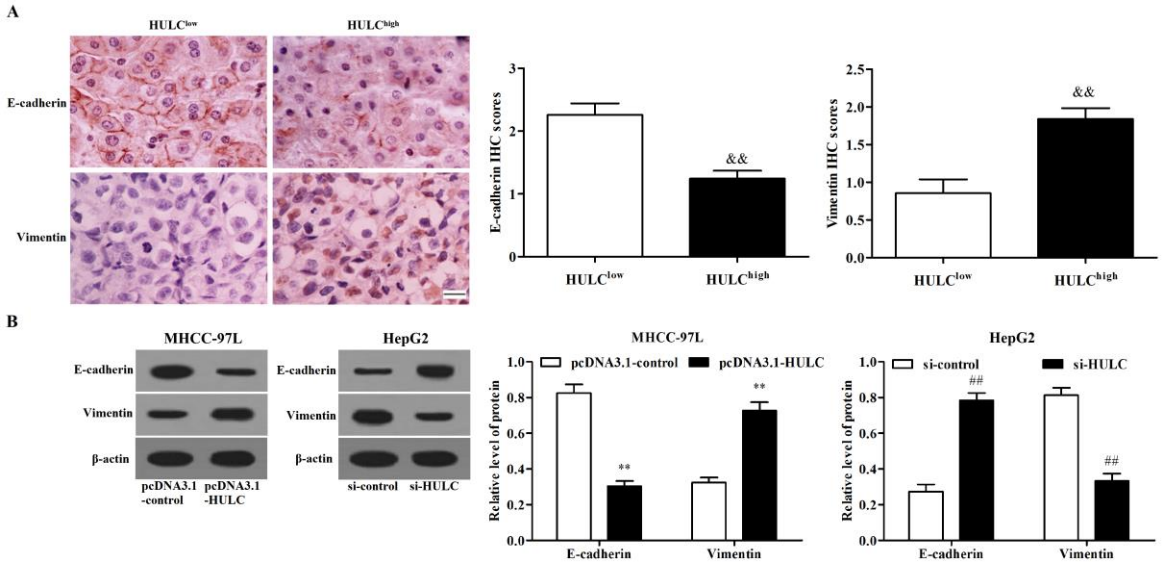

Figure 4. MiR-372 expression in HCC tissues and cells and its relationship with HULC. (A) Binding sites between miR-372 and HULC. Results of qRT-PCR analysis showing miR-372 expression in (B) HCC and normal liver tissues, and (C) HCC cell lines. (D) Pearson correlation analysis showing a negative correlation between miR-372 and HULC. (E) MiR-372 expression levels in HCC cells transfected with miR-372 mimics or inhibitor. (F) Luciferase activity in cells transfected with miR-372 and HULC 3'UTR wt/mut. (G) Mir-372 expression levels in HCC cells overexpressing HULC. (H) HULC expression in HCC cells expressing miR-372 mimics or inhibitor. $^{\#\#}$P<0.01 compared to nontumor group, $^{\&\&}$P<0.01, $^{\&\&\&}$P<0.001 compared to LO2 group, *p<0.05, **p<0.01 compared to NC group, $^{\theta\theta}$P<0.01 compared to pcDNA3.1-control group, and $^{\delta}$P<0.05 compared to si-control group.

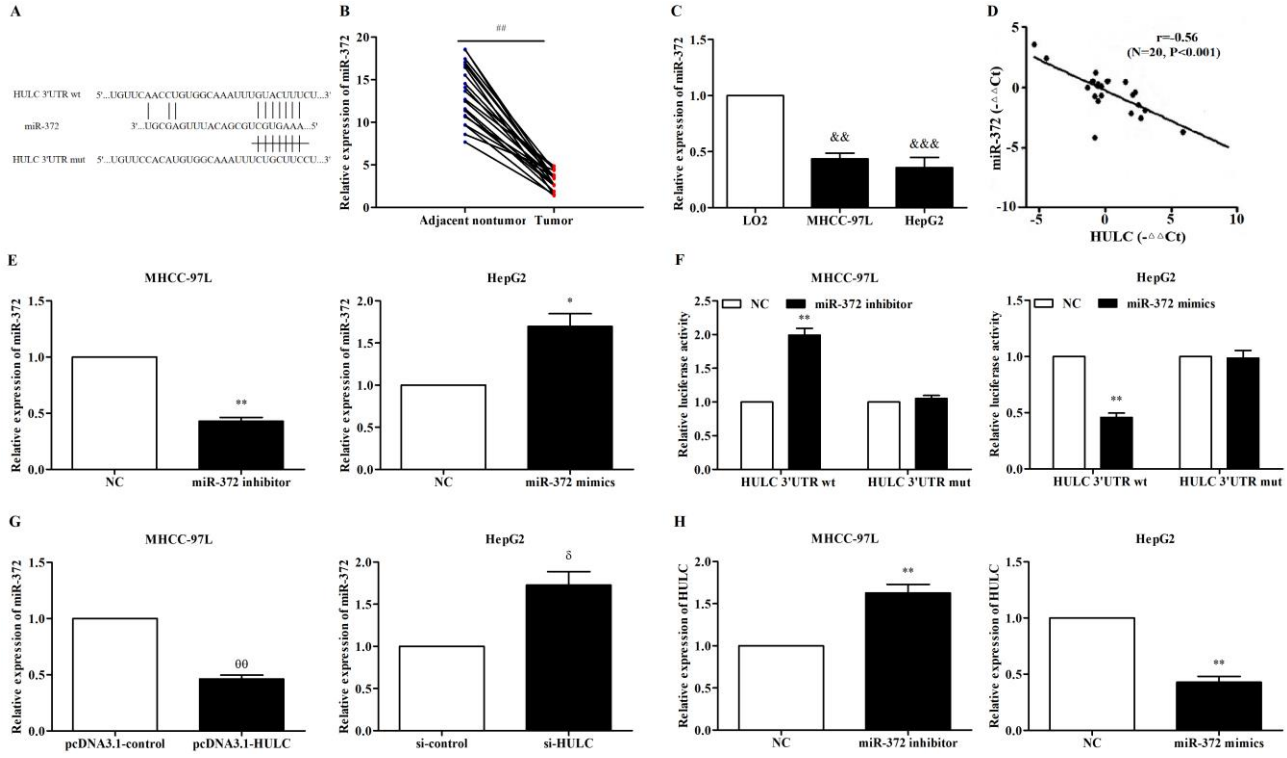

Figure 5. MiR-372 inhibits proliferation and promotes apoptosis of HCC cells. (A) Percentage of viable MHCC-97L and HepG2 cells respectively transfected with miR-372 inhibitor and mimics. (B) Number of colonies formed by the low and high miR-372 expressing cells. (C) Flow cytometry plots indicating the apoptosis rates in low and high miR-372 expressing cells. $^{*}P<0.05$ and $^{**}p<0.01$ compared to NC group.

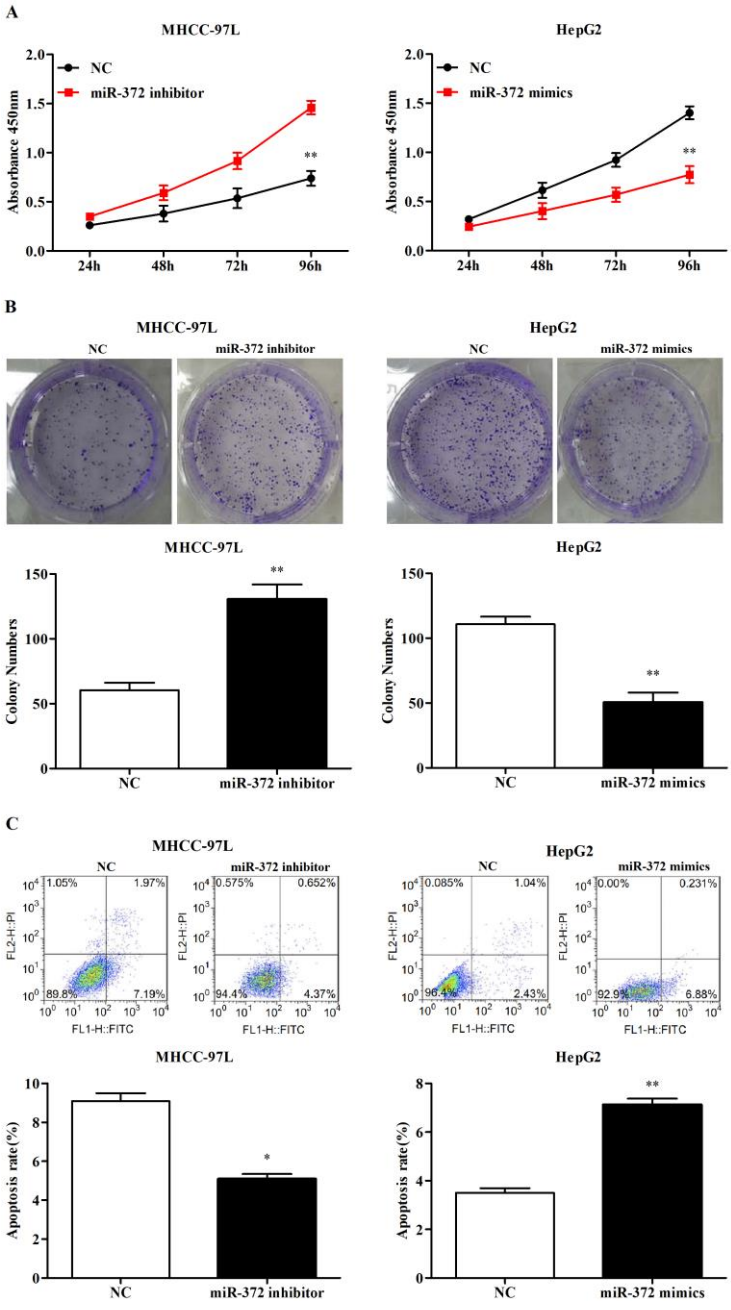

Figure 6. MiR-372 inhibits EMT progression of HCC cells. (A) Representative IHC images showing in situ expression of E-cadherin and Vimentin in the low and high miR-372 expressing cells (x400). (B) Immunoblot showing E-cadherin and Vimentin expression levels in the suitably transfected MHCC-97L and HepG2 cells. $^{\&\&}$P<0.01 compared to miR-372^{high} group, **p<0.01 and ***P<0.001 compared to NC group.

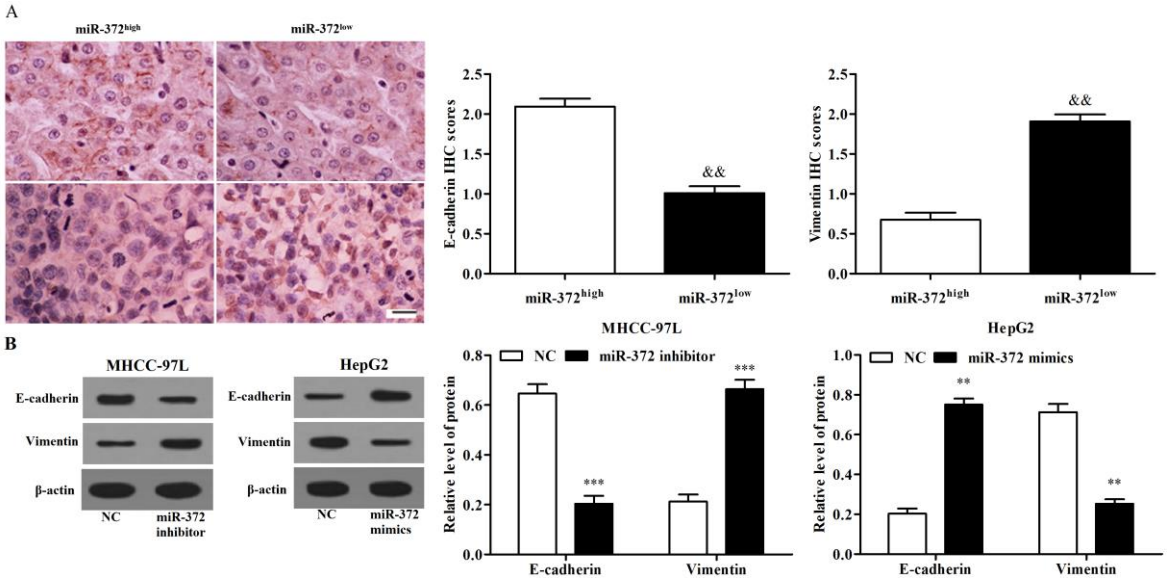

Figure 7. CXCR4 expression in HCC tissues and cells and its relationship with miR-372. (A) Binding site between miR-372 and CXCR4. Results of qRT-PCR indicating CXCR4 mRNA levels in (B) tumor and normal tissues, and (C) HCC cell lines. (D) Pearson correlation analysis showing negative correlation between miR-373 and CXCR4. (E) Luciferase activity in HCC cells expressing miR-372 and CXCR4 3'UTR wt/mut. CXCR4 levels in HCC cells overexpressing (F) miR-372 and (G) HULC. $^{\#\#}$P<0.01 compared to nontumor group, $^{\&}$P<0.05 and $^{\&\&}$P<0.01 compared to LO2 group, **P<0.01 compared to NC group, $^{\wedge\wedge}$P<0.01 compared to pcDNA3.1-control group, and $^{\theta\theta}$P<0.01 compared to si-control group.

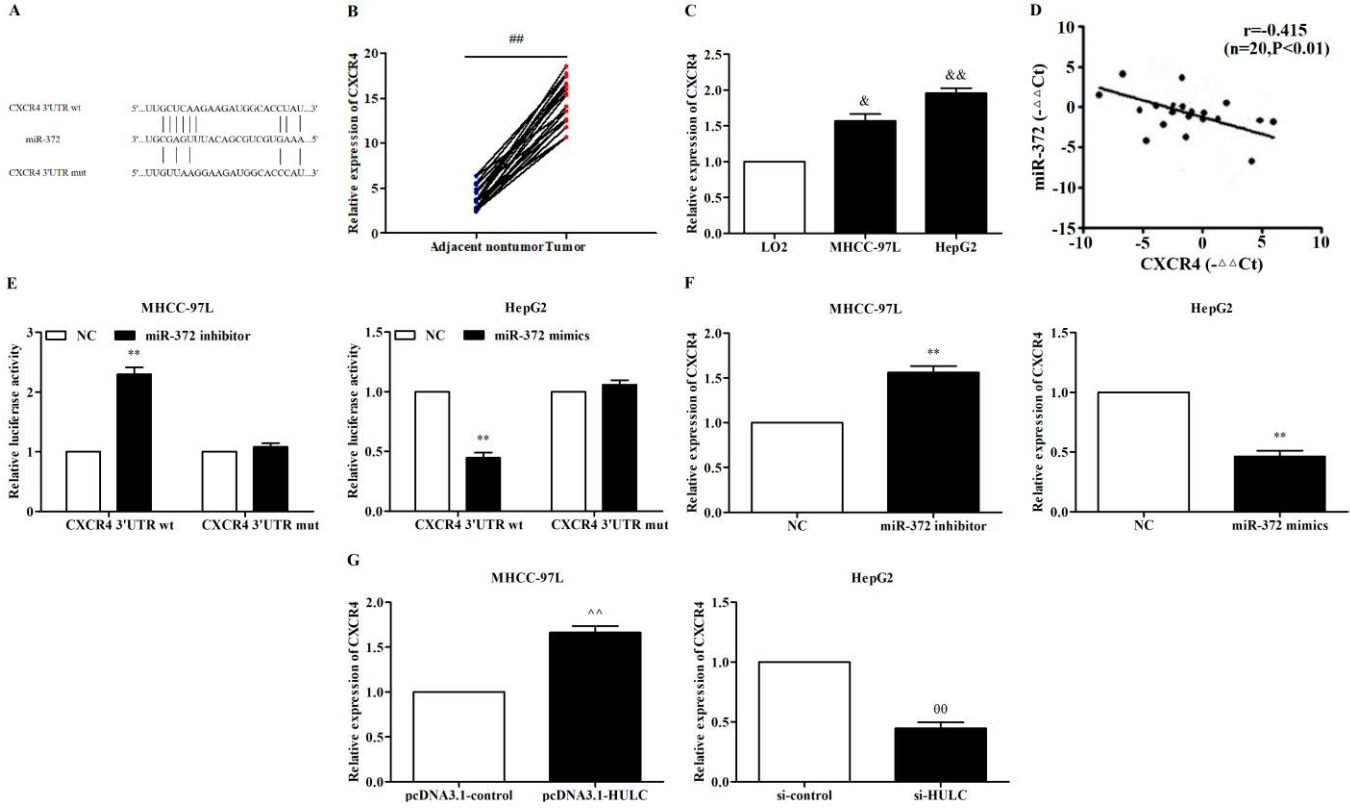

Figure 8. HULC/miR-372/CXCR4 axis regulates HCC cell proliferation, apoptosis and EMT. (A) The results of qRT-PCR showing CXCR4 expression levels in HULC and miR-372-overexpressing MHCC-97L cells and HULC and miR-372-silenced HepG2 cells. (B) Viability, (C) proliferation and (D) apoptosis rates in the indicated cells. (E) Immunoblot showing E-cadherin and Vimentin levels in the indicated cells. $^{**}P<0.01$ $^{***}P<0.001$ compared with pcDNA3.1-control group, $^{\#}P<0.05$, $^{\#\#}P<0.01$ and $^{\#\#\#}P<0.001$ compared to si-control group

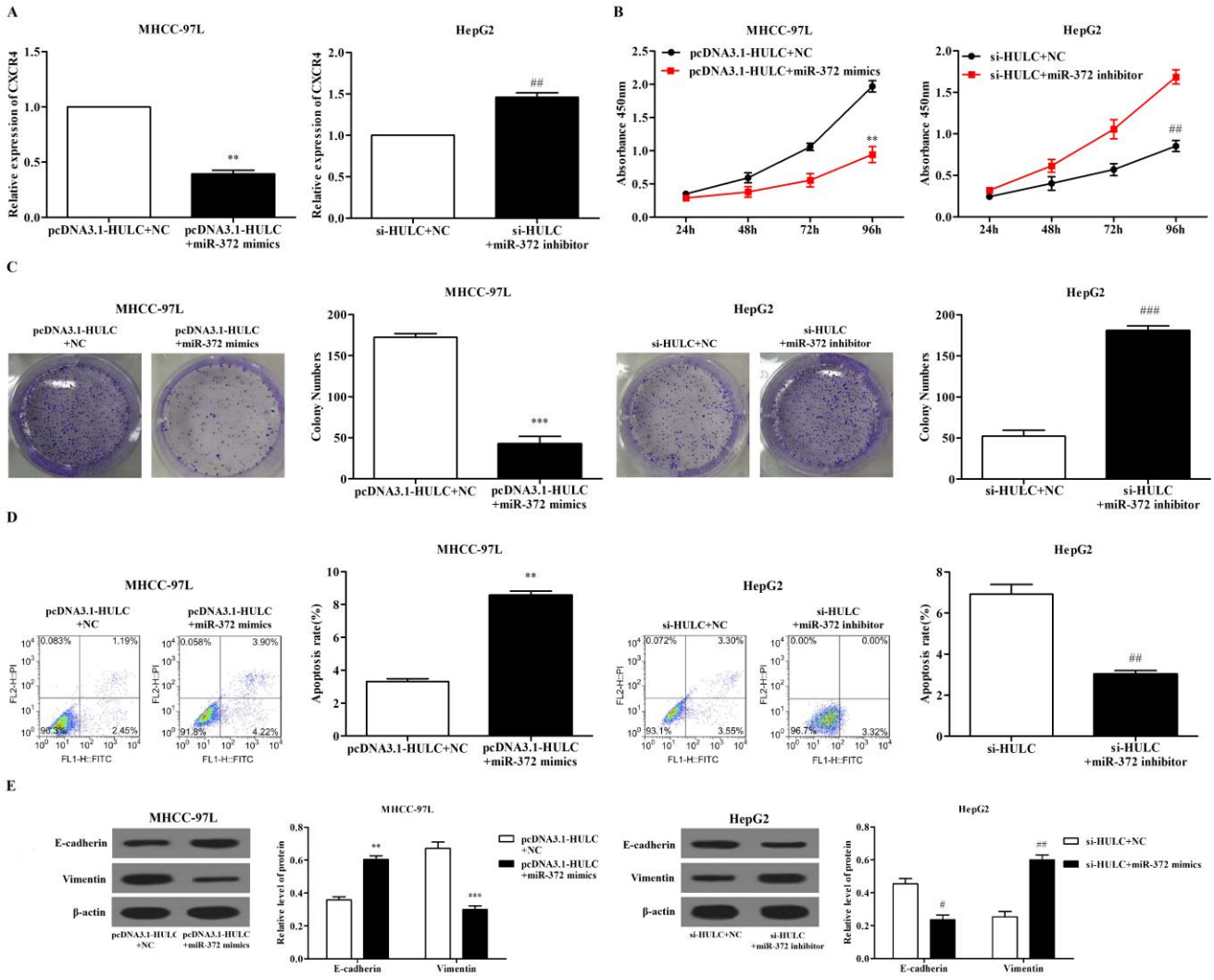

Figures

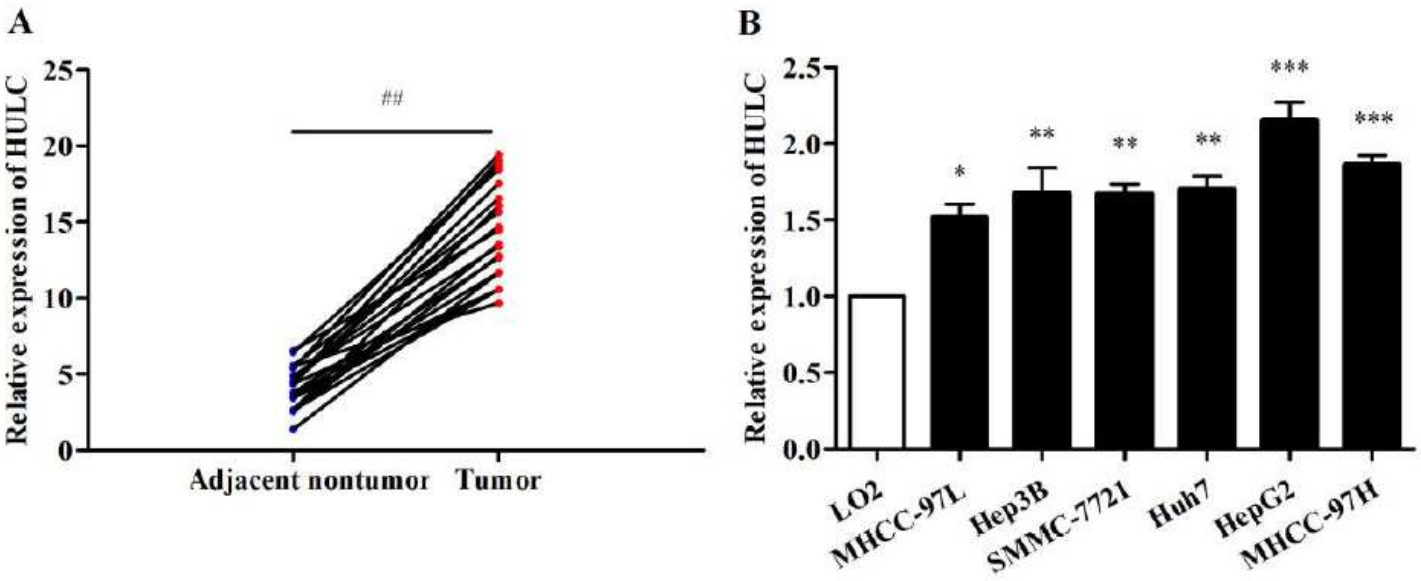

Figure 1

HULC expression in HCC tissues and cells. The results of qRT-PCR analysis showing upregulation of HULC in (A) tumor and adjacent non-tumor tissues, and (B) HCC cell lines and LO2 cells. ##P<0.01 compared to adjacent non-tumor tissues, *P<0.05, **P<0.01 and ***P<0.001 compared to LO2 cells.

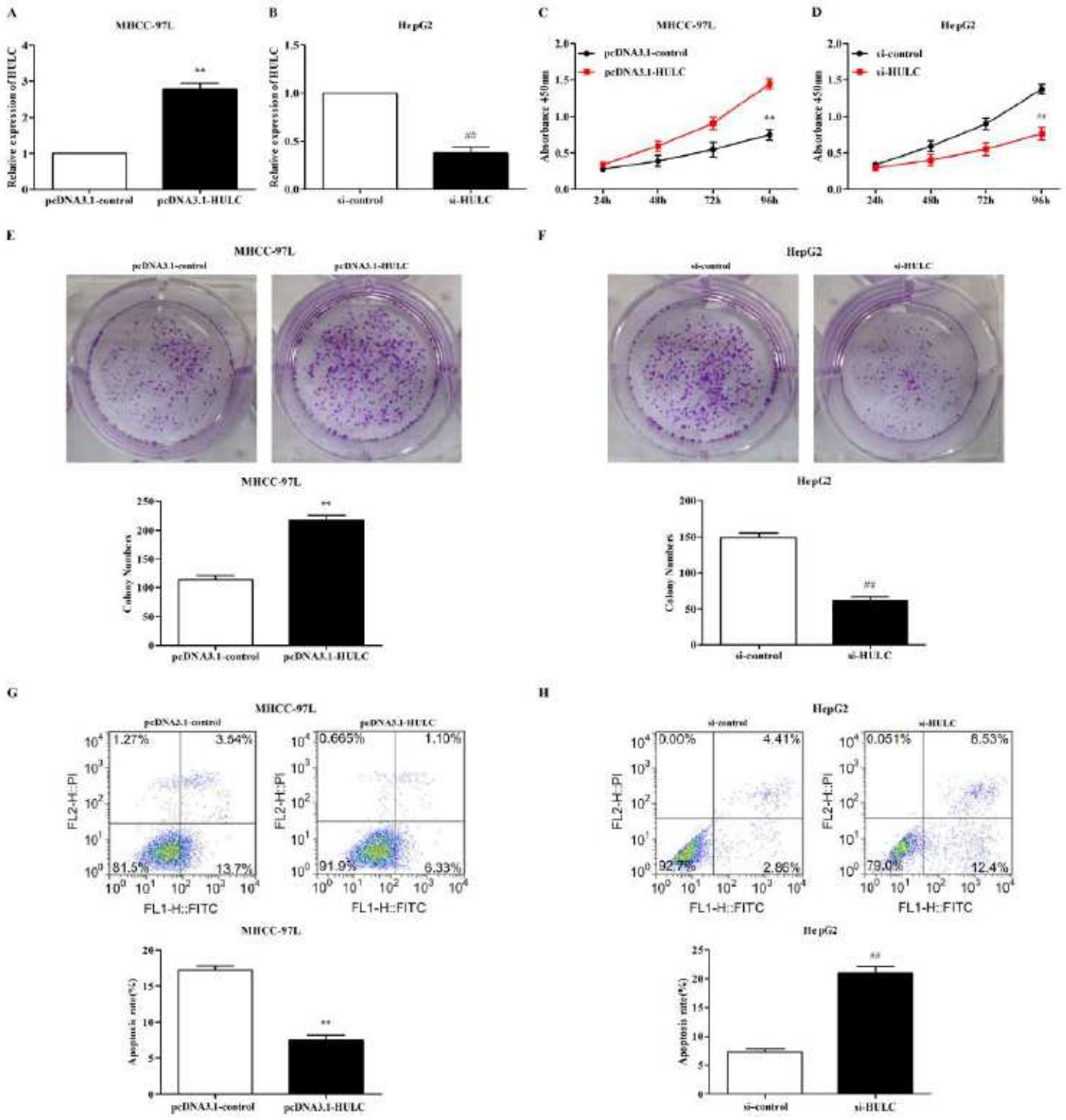

Figure 2

HULC enhances the neoplastic characteristics of HCC cells. Results of qRT-PCR analysis showing HULC expression levels in (A) MHCC-97L and (B) HepG2 cells. CCK-8 assay showing the effect of (C) pcDNA3.1-HULC and (D) si-HULC on the viability of indicated HCC cell lines. Number of colonies formed by the (E) HULC-overexpressing MHCC-97L cells and (F) HULC knockdown HepG2 cells. Flow cytometry plots showing apoptosis rates in (G) HULC-overexpressing MHCC-97L cells and (H) HULC knockdown HepG2

cells. **P<0.01 compared with the pcDNA3.1-control group, and ##P<0.01 compared with the si-control group.

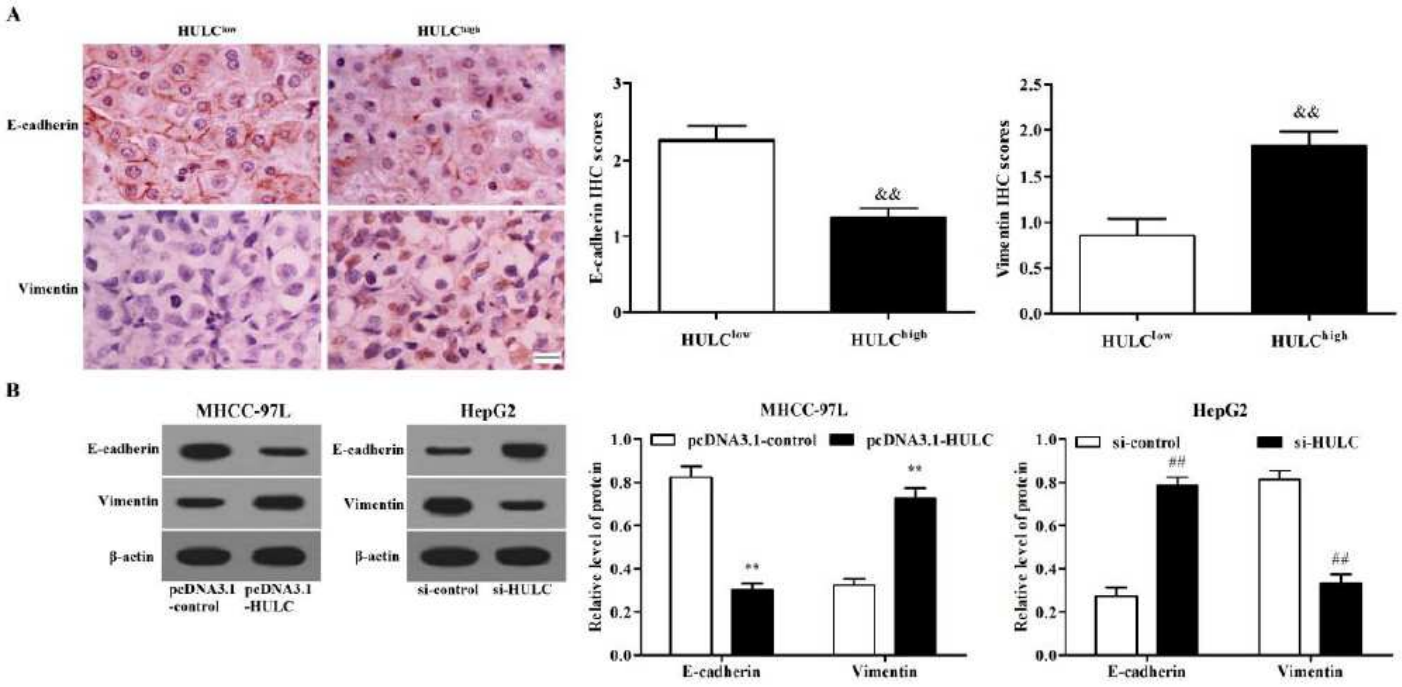

Figure 3

HULC promoted EMT progression of HCC cells. (A) Representative IHC images showing in situ E-cadherin and Vimentin expression in the HULC-overexpressing and HULC-knockdown HCC cells (x400). (B) Immunoblot showing expression levels of E-cadherin and Vimentin in the indicated cell lines. &&P<0.01 compared to HULClow group, **p<0.01 compared to pcDNA3.1-control group, and ##P<0.01 compared to si-control group.

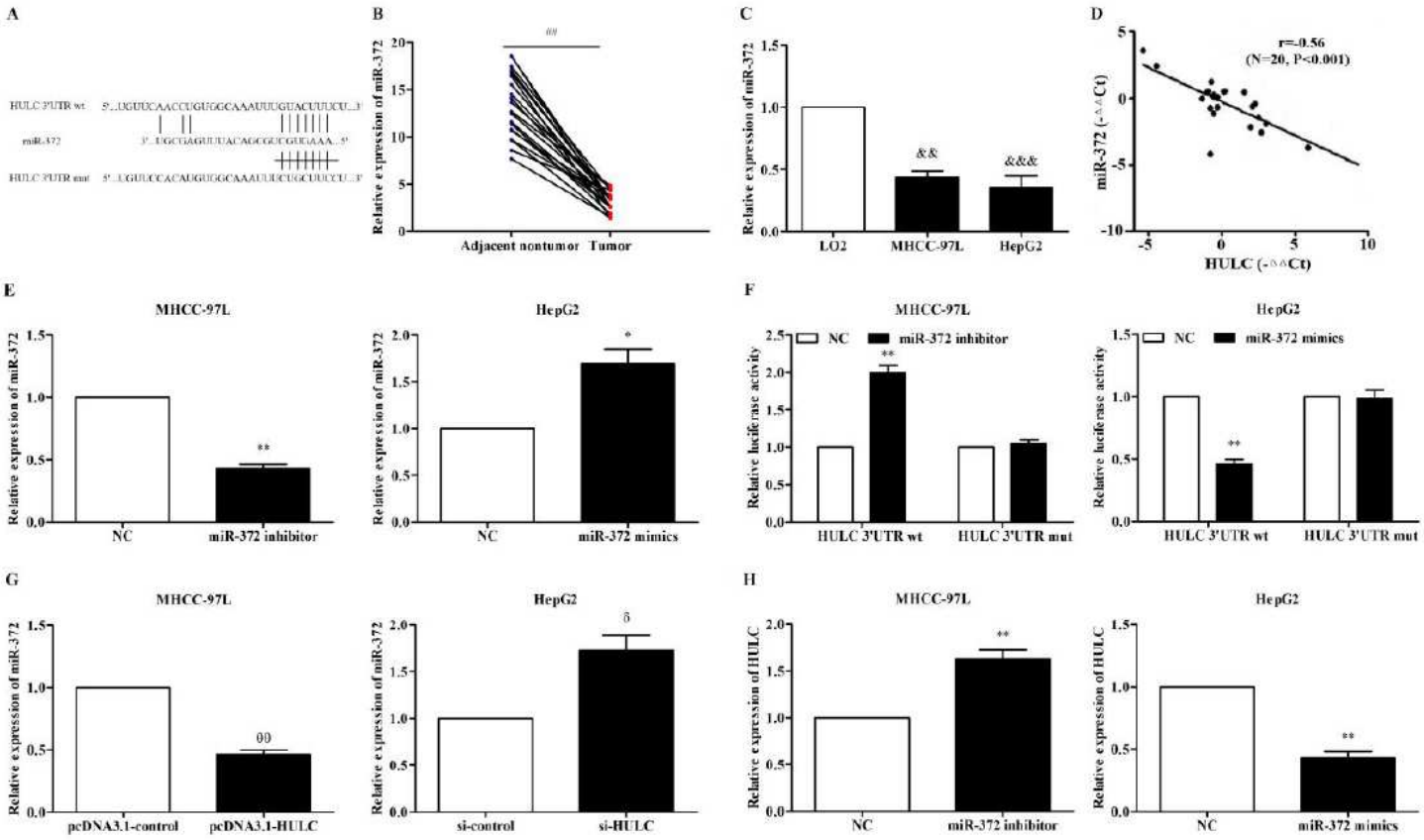

Figure 4

MiR-372 expression in HCC tissues and cells and its relationship with HULC. (A) Binding sites between miR-372 and HULC. Results of qRT-PCR analysis showing miR-372 expression in (B) HCC and normal liver tissues, and (C) HCC cell lines. (D) Pearson correlation analysis showing a negative correlation between miR-372 and HULC. (E) MiR-372 expression levels in HCC cells transfected with miR-372 mimics or inhibitor. (F) Luciferase activity in cells transfected with miR-372 and HULC 3'UTR wt/mut. (G) Mir-372 expression levels in HCC cells overexpressing HULC. (H) HULC expression in HCC cells expressing miR-372 mimics or inhibitor. ##P<0.01 compared to nontumor group, &&P<0.01, &&&P<0.001 compared to LO2 group, *p<0.05, **p<0.01 compared to NC group, θθP<0.01 compared to pcDNA3.1-control group, and δP<0.05 compared to si-control group.

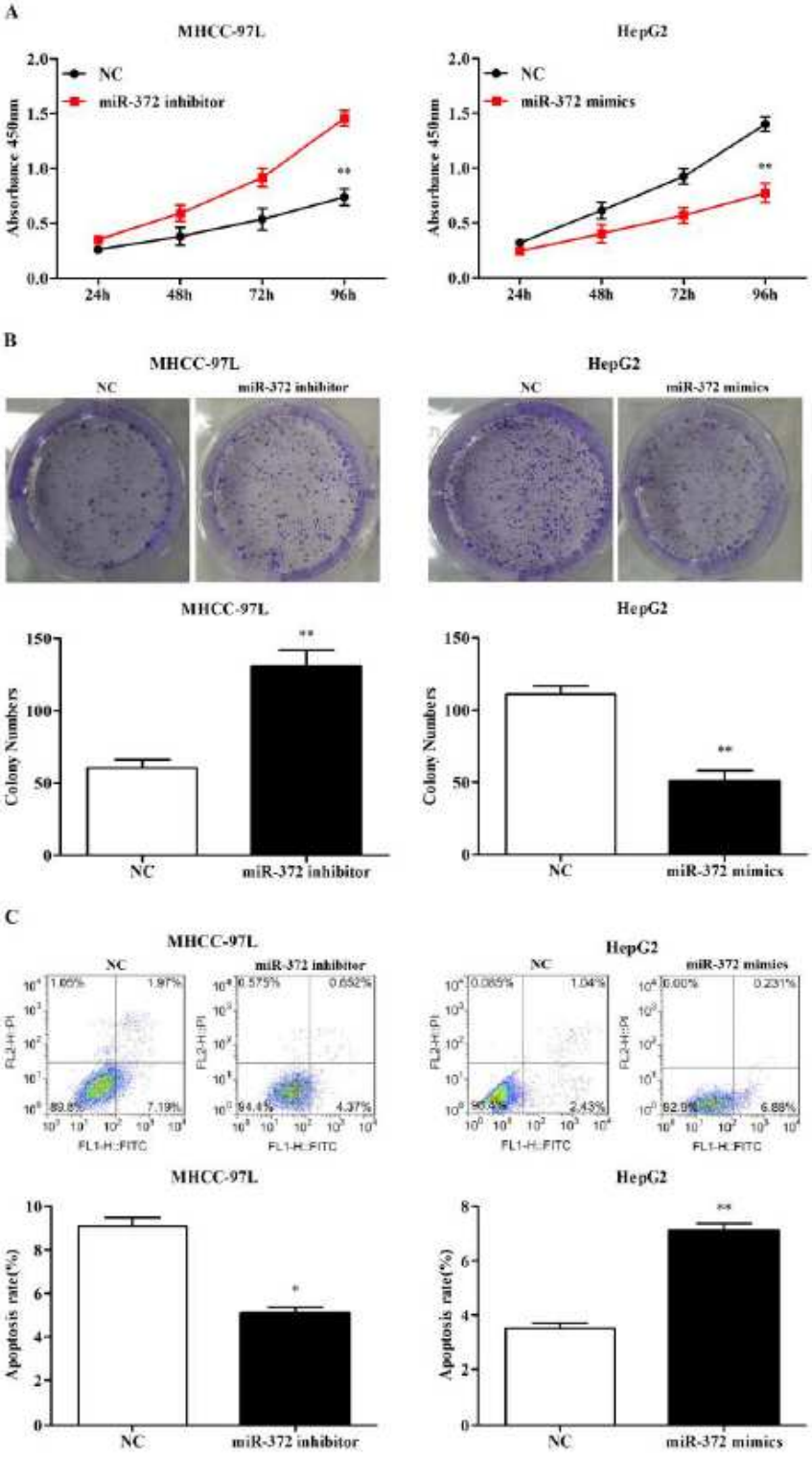

Figure 5

MiR-372 inhibits proliferation and promotes apoptosis of HCC cells. (A) Percentage of viable MHCC-97L and HepG2 cells respectively transfected with miR-372 inhibitor and mimics. (B) Number of colonies formed by the low and high miR-372 expressing cells. (C) Flow cytometry plots indicating the apoptosis rates in low and high miR-372 expressing cells. *P<0.05 and **p<0.01 compared to NC group.

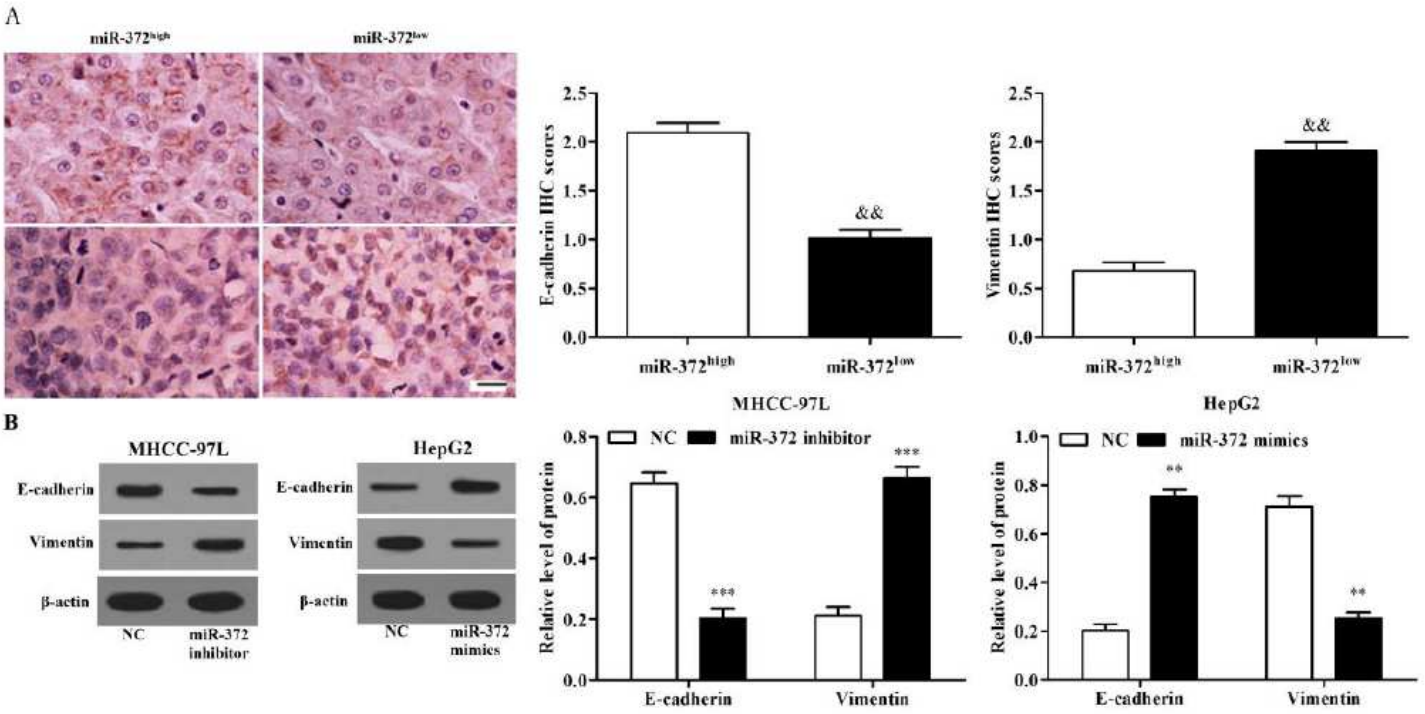

Figure 6

MiR-372 inhibits EMT progression of HCC cells. (A) Representative IHC images showing in situ expression of E-cadherin and Vimentin in the low and high miR-372 expressing cells (x400). (B) Immunoblot showing E-cadherin and Vimentin expression levels in the suitably transfected MHCC-97L and HepG2 cells. &&P<0.01 compared to miR-372high group, **p<0.01 and ***P<0.001 compared to NC group.

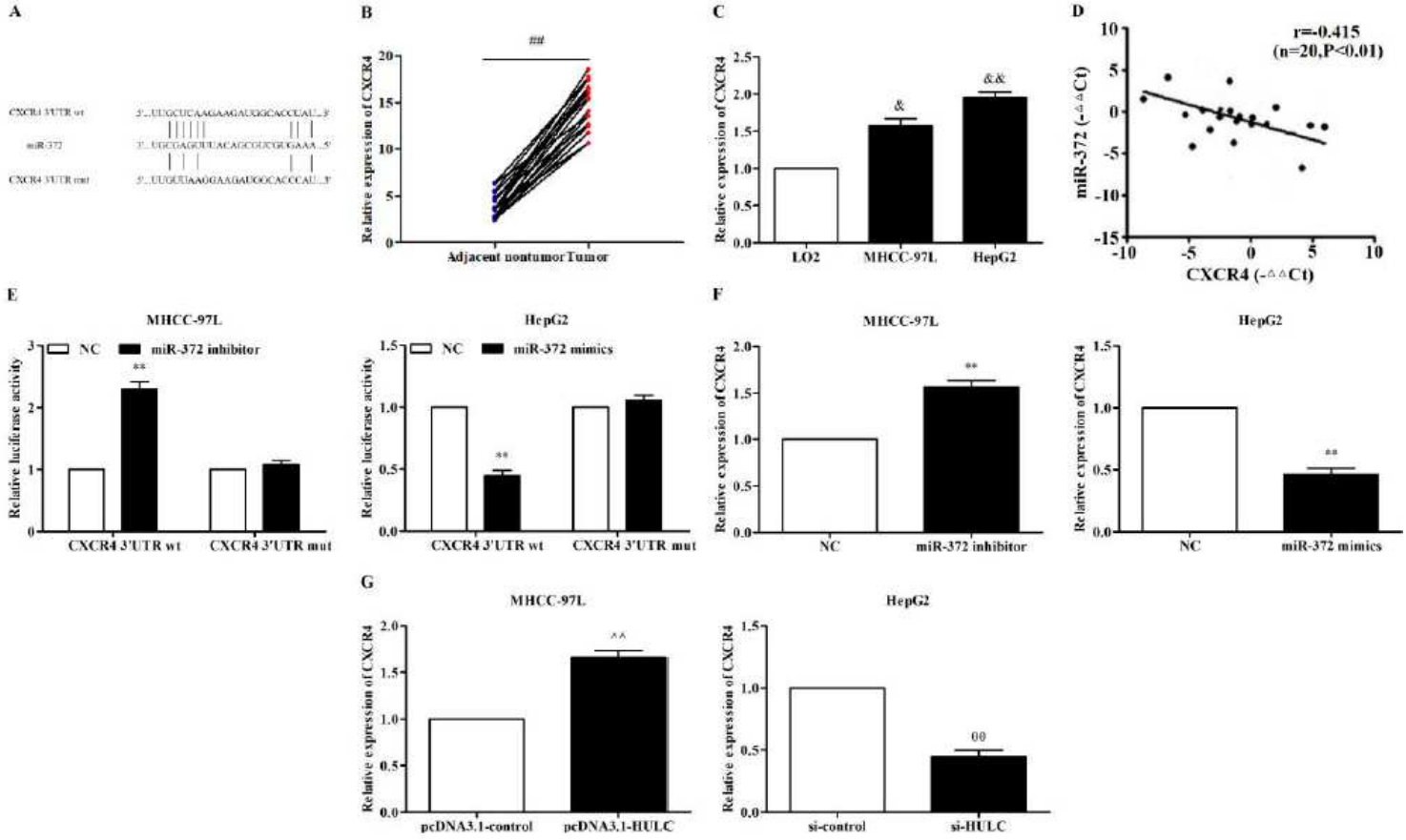

Figure 7

CXCR4 expression in HCC tissues and cells and its relationship with miR-372. (A) Binding site between miR-372 and CXCR4. Results of qRT-PCR indicating CXCR4 mRNA levels in (B) tumor and normal tissues, and (C) HCC cell lines. (D) Pearson correlation analysis showing negative correlation between miR-373 and CXCR4. (E) Luciferase activity in HCC cells expressing miR-372 and CXCR4 3'UTR wt/mut. CXCR4 levels in HCC cells overexpressing (F) miR-372 and (G) HULC. ##P<0.01 compared to nontumor group, &P<0.05 and &&P<0.01 compared to LO2 group, **P<0.01 compared to NC group, ^^P<0.01 compared to pcDNA3.1-control group, and θθP<0.01 compared to si-control group.

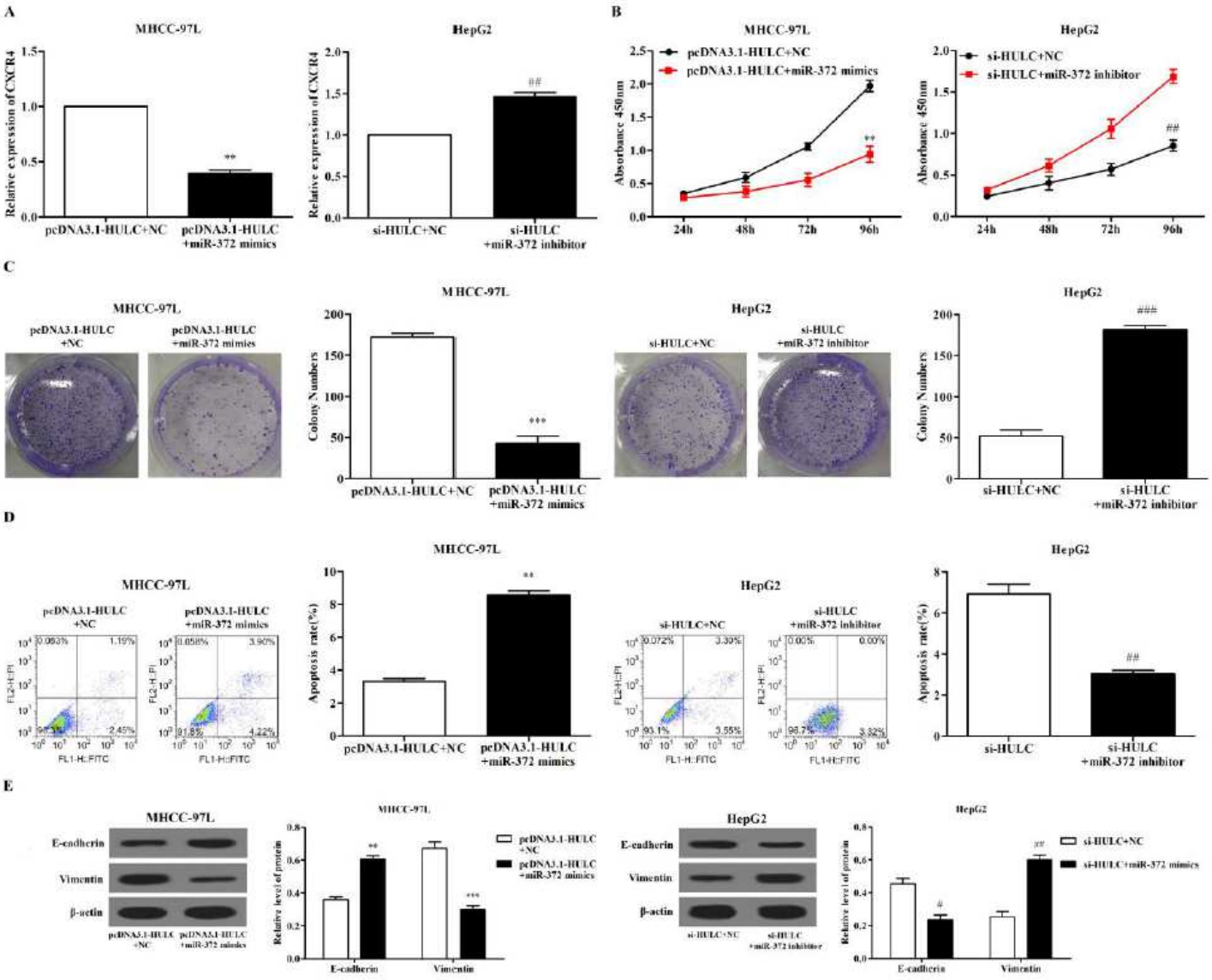

Figure 8

HULC/miR-372/CXCR4 axis regulates HCC cell proliferation, apoptosis and EMT. (A) The results of qRT-PCR showing CXCR4 expression levels in HULC and miR-372-overexpressing MHCC-97L cells and HULC and miR-372-silenced HepG2 cells. (B) Viability, (C) proliferation and (D) apoptosis rates in the indicated cells. (E) Immunoblot showing E-cadherin and Vimentin levels in the indicated cells. **P<0.01 ***P<0.001 compared with pcDNA3.1-control group, #P<0.05, ##P<0.01 and ###P<0.001 compared to si-control group